Conference Proceedings

EuroSun 2014
Aix-les-Bains (France), 16 – 19 September 2014

BISCHOFITE AS PHASE CHANGE MATERIAL (PCM) FOR THERMAL ENERGY STORAGE (TES) APPLICATIONS

Jaume Gasia[1], Andrea Gutierrez[2], Laia Miró[1], Gerard Peiró[1], Svetlana Ushak[2,3] and Luisa F Cabeza[1]

[1] GREA Innovació Concurrent, Universitat de Lleida, edifici CREA, Pere de Cabrera s/n, 25001 Lleida (Spain)

[2] Department of Chemical Engineering and Mineral Processing and Center for Advanced Study of Lithium and Industrial Minerals (CELiMIN). Universidad de Antofagasta, Campus Coloso, av. Universidad de Antofagasta, 02800 Antofagasta (Chile)

[3] Solar Energy Research Center (SERC-Chile), University of Chile, Av Tupper 2007, Piso 4, Santiago, Chile

Abstract

Bischofite is a by-product from the non-metallic industry which is composed by $MgCl_2 \cdot 6H_2O$ in approximately 95%. Both materials show similar thermo-physical properties, the temperature and the heat of fusion is 100°C and 115 kJ/kg for bischofite, and 114.5°C and 135 kJ/kg for $MgCl_2 \cdot 6H_2O$. The main advantage of the use of bischofite instead of $MgCl_2 \cdot 6H_2O$ is the price, which is significantly lower. The present study consists in two stages: in the first one, a laboratory characterization of thermal properties such as melting enthalpy and temperature, heat capacity, as well as density, viscosity and its morphology is performed. In the second stage, the material is tested and evaluated at pilot plant scale (≈ 200 kg). Parameters such as the phase change material (PCM) charging temperatures, the HTF power, the energy balance in the system and the charging efficiency are analysed. Moreover, this PCM candidate is also compared with other materials with similar melting temperature (± 20 ºC) regarding the cost and the energy density. Finally, taking into account bischofite temperature of fusion (100 ºC), a discussion of its utilization for industrial waste heat recovery or combined heat and power (CHP) possibilities is done. Thus, the objective of this study is the analysis of the suitability of a by-product as PCM candidate for thermal energy storage (TES) applications.

Key-words: bischofite, phase change material (PCM), thermal energy storage (TES), by-product, latent heat.

1. Introduction

According to the International Energy Agency (IEA) (2014), current trends in energy supply and use are economically, environmentally and socially unsustainable: energy-related emissions of carbon dioxide will double by 2050 and fossil energy demand will increase over the security of supplies. Moreover, IEA states that energy storage technologies can support energy security and climate change goals.

Regarding into thermal energy storage, latent heat storage has been widely studied previously using highly pure thermal energy storage (TES) materials like paraffin and salt hydrates (Zalba et al., 2003; Mehling and Cabeza, 2008). However, by-products or waste materials from different industrial sectors that have also potential to be applied as TES materials are starting to be studied (Miró et al., 2014). The main advantage of the use of this material is their availability and lower price comparing them to pure materials.

In the case of the enormous non-metallic industry in North of Chile, they obtain nitrates, carbonates, sulphates, chlorides and other salts from the Atacama Desert salt flat and mineral rocks on a large scale. Some of these productive processes leave salts as by-products or waste materials. Bischofite is one of these salts; it precipitates in the evaporations brines, during the obtaining process of Li_2CO_3. Bischofite is a hydrated salt mainly composed by $MgCl_2 \cdot 6H_2O$ (95% and the rest are impurities), with thermal properties similar to synthetic $MgCl_2 \cdot 6H_2O$ (Ushak et al., 2014). It is now been applied for the de-icing of roads, and also in Chile, due to its hygroscopicity is use to abate dust and to improve mining roads in the North region, and it has become interesting because this salt is available in huge amounts and is also cheaper: the price of low quality bischofite is around 40 US$/ton, while the price of purified bischofite is closed but lower to that of $MgCl_2 \cdot 6H_2O$, which is sold at around 155 US$/ton in the north of Chile (Ushak et al., 2014).

Taking into account the advantages of bischofite as TES material, the objective of this study is to evaluate the

© 2015. The Authors. Published by International Solar Energy Society
Selection and/or peer review under responsibility of EuroSun2014 Scientific Committee
doi:10.18086/eurosun.2014.10.03 Available at http://proceedings.ises.org

real potential of this by-product at laboratory and pilot plant scale (≈ 200 kg) as phase change material (PCM) as well as comparing it with other PCM with similar temperature of fusion (± 20 ºC) regarding the cost and the energy density and, finally, to review possible applications for this new PCM.

2. Laboratory analysis

At laboratory scale, the thermo-physical properties of bischofite are determined. Regarding to the physical characterization, mineral composition, morphology, density in solid and liquid state and viscosity are determined. Focusing on the thermal properties, melting temperature, heat of fusion and heat capacity in solid and liquid state are studied.

The results of the mineralization study of the bischofite (Figure 1, right), according to stoichiometric calculations based on chemical analysis, shows that it is composed around 95 % of $MgCl_2 \cdot 6H_2O$ and the remaining 5 % is potassium carnalite, lithium sulphate monohydrate, and ionic salts like NaCl and KCl (Ushak et al., 2014). Due to the similarity in their composition, from now on, properties of bischofite are listed together with $MgCl_2 \cdot 6H_2O$.

Element	Average concentration range [%]
Sodium, Na	0.321 – 0.360
Potasium, K	0.259 – 0.301
Calcium, Ca	0.007 – 0.008
Magnesium, Mg	10.84 – 11.45
Lithium, Li	0.298 – 0.351
Chloride, Cl	33.66 – 34.92
Sulfate, SO_4	1.29 – 1.51
Moisture	1.42 – 1.50

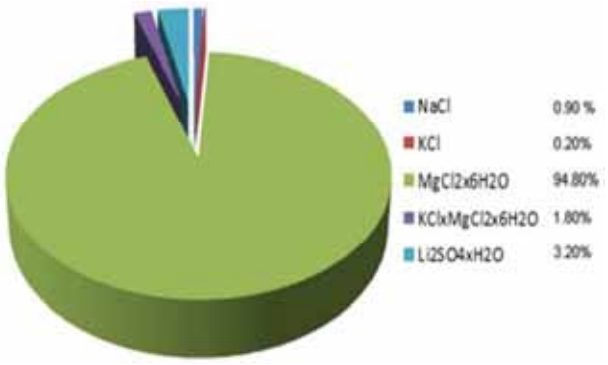

Fig. 1: Chemical composition (left) and mineralization (right) of bischofite (Ushak et al., 2014)

Viscosity was determined for the liquid phase of bischofite and $MgCl_2$ $6H_2O$. As it can be observed in figure 2 viscosity decreases while temperature is increasing, reducing in almost 50% from 105 ºC to 150 ºC. Finally, density in both states and for both materials was measured pycnometrically (Table 1).

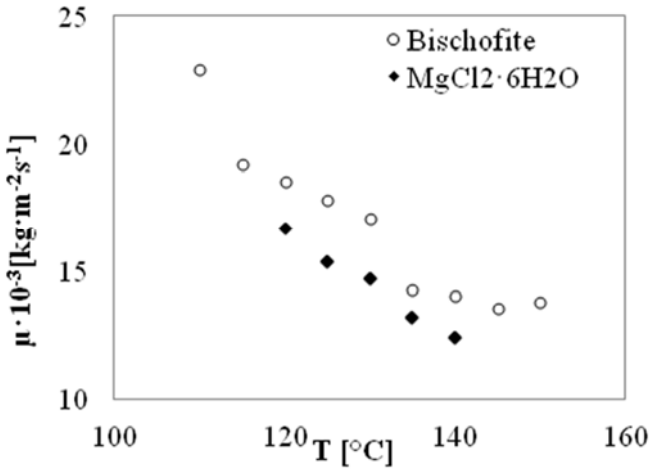

Fig. 2: Dynamic viscosity for liquid phase of bischofite and $MgCl_2$ $6H_2O$ (Ushak et al., 2014)

Tab. 1: Density in solid and liquid state for bischofite and $MgCl_2 \cdot 6H_2O$ (Ushak et al., 2014)

	Units	Bischofite	$MgCl_2 \cdot 6H_2O$
Density in solid state (ρ_s)	[g/cm^3]	1686 -1513	1517
Density in liquid state (ρ_l)	[g/cm^3]	1481	1422

Thermophysical properties of bischofite and synthetic $MgCl_2 \cdot 6H_2O$ (Table 2), are very similar, with slight differences due to, mainly, the presence of impurities in bischofite composition (Figure 1, right). Focusing on the thermal performance in DSC analysis (Figure 3), it was observed that both salts present an appreciable subcooling (37 ºC for bischofite and 29 ºC for $MgCl_2 \cdot 6H_2O$), which is a disadvantage when applying these salts as a PCM.

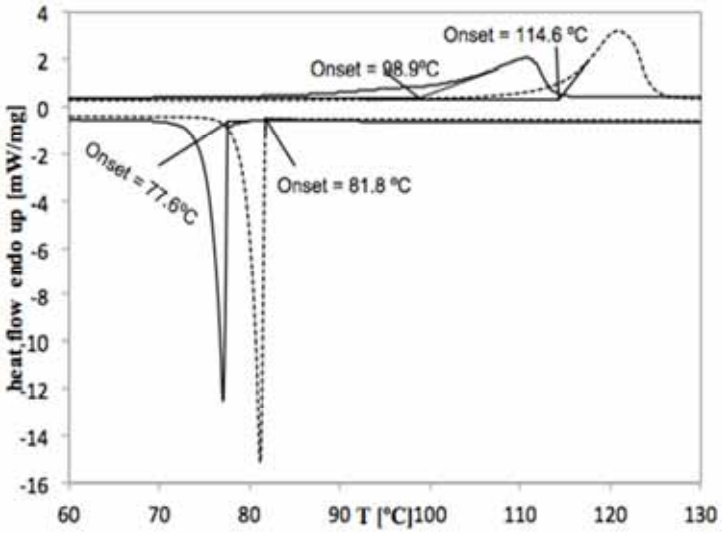

Fig. 3: Cycle of heating and cooling for bischofite (continuous line) and synthetic $MgCl_2 \cdot 6H_2O$ (dotted line) (Ushak et al., 2014)

Tab. 2 Summary of thermophysical properties for bischofite and $MgCl_2 \cdot 6H_2O$ (Ushak et al., 2014)

Properties	Units	Bischofite	$MgCl_2 \cdot 6H_2O$
Melting temperature (T_m)	[ºC]	100	114.5
Melting enthalpy (H_m)	[kJ/kg]	115	135
Heat capacity in solid state at 25-60ºC (Cp_s)	[kJ/kg·K]	2.1	1.95-2.1

3. Possible applications

Thermal properties of this material, and specially its temperature of fusion (100 ºC), make it a candidate for industrial waste heat (IWH) recovery as well as for combined heat and power (CHP) facilities.

For IWH recovery, the use of bischofite in passive technologies as thermal energy storage (Brueckner et al., 2014) is proposed. In table 3, the exhaust gas temperatures of different industrial processes are listed. These exhaust gas temperature could be stored in bischofite for a later use.

Tab. 3 Exhaust gas temperature of different industrial processes, based on (Brueckner et al., 2014)

Process	Exhaust gas temperature (°C)
Steam boiler	200 – 300
Coke oven / Stack gas	190
Container glass melting	160 – 200 / 140 – 160
Flat glass melting	160 – 200 / 140 – 160
Ceramic kiln	150 – 1000
Drying, baking, and curing ovens	90 – 230
Cooling water from annealing furnaces	70 – 230
Cooling water from internal combustion engines	70 – 120
Exhaust gases exiting recovery devices in gas-fired boilers, ethylene furnaces, etc.	70 - 230
Conventional hot water boiler	60 – 230

4. Comparison with other PCM candidates ≈ 100 ºC

In figure 4, bischofite is compared with other organic and inorganic phase change temperature materials with a T_m = ± 20 ºC: acetamide (T_m= 82 ºC), $Mg(NO_3)_2 \cdot 6H2O$ (T_m= 89 ºC), xylitol (T_m= 93-94.5 ºC), d-Sorbitol (97.7 ºC), $MgCl_2 \cdot 6H_2O$ (T_m=117 ºC) and erythritol (T_m=118 ºC) (Cabeza et al., 2011; Sharma et al., 2002; Kenisarin et al., 2007). The parameters compared are energy density and cost. A PCM will be more suitable for an application when the lower the cost and the higher the energy density. An arrow point to the optimum area represented in figure 4.

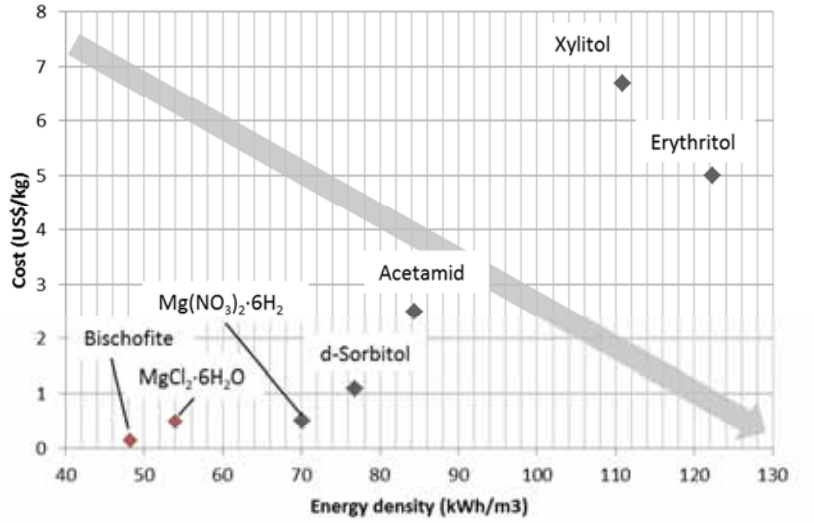

Fig. 2: Cost and energy density for some PCM, based on Cabeza et al. (2011), Kenisarin et al. (2007), Stevens (2013), and Ushak et al. (2014)

5. Pilot plant testing

The facility used to perform the experimentation presented in this study and to evaluate the behaviour of bischofite as PCM at pilot plant scale is located at the University of Lleida and is mainly composed of three parts: the heating system, the cooling system and the storage system (Figure 5). The heating system consists of an electrical boiler of 24 $KW_{e,}$ that heat the heat transfer fluid (HTF) up simulating the solar energy source during the charging process, the cooling system consists of a an air-HTF heat exchanger of 20 kW_{th} simulating the energy consumption in a real installation during the discharging process, and the storage systems consisting on a storage tank which mission is to store the energy during the charging process and released during the discharging process. Silicone Syltherm-800 was used as HTF and all the piping that connects the different systems are insulated using rock wool. Moreover, measuring equipment is placed around the installation in

order to control and acquire information and data related to the HTF flow rate, HTF temperatures and HTF pressures.

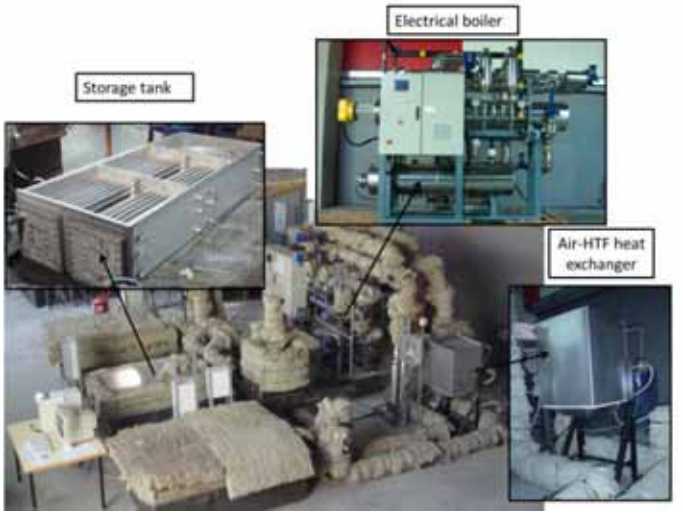

Fig. 5 Pilot plant facility at the University of Lleida (Gil et al., 2013)

Focusing on the storage tank, the one used to perform the present experimentation is based on the shell-and-tubes heat exchanger concept, consisting of a stainless steel vessel, where the PCM is placed, which houses 49 tubes bended in U shape and distributed in square pitch. Moreover, 450 mm of foamglass are installed between the tank and the floor and 240 mm of rock wool are installed on the lateral walls and on the cover of the tank to reduce the heat losses to the surroundings. Table 4 shows the main characteristics of the storage tank.

Tab. 4: Main characteristics of the storage tank

Parameters	Units	Values
Tank width	[mm]	527.5
Tank height	[mm]	273
Tank depth	[mm]	1273
HTF pipes average length	[mm]	2485
Heat transfer surface	[m^2]	6.55
Tank vessel volume (V_{tank})	[m^3]	0.154
Real volume of PCM (V_{PCM})	[m^3]	0.143
PCM mass	[kg]	204
Packing factor (V_{PCM}/V_{tank})	[-]	0.837

So as to study and evaluate the thermal behaviour of PCM inside the tank (from $T_{PCM.1}$ to $T_{PCM.15}$ in figure 6: right) 19 temperature sensors PT-100 with an accuracy of ± 0.1 ºC were placed in the main part of the tank. Moreover, 16 more temperature sensors were placed to study the behaviour of the PCM in the corners and central part as well as to study the heat losses. These sensors are located within the tubes bundle and distributed in three different heights, at 31 mm, 126 mm and 190 mm from the bottom of the tank and with three different lengths: 35 mm, 114 mm and 194 mm.

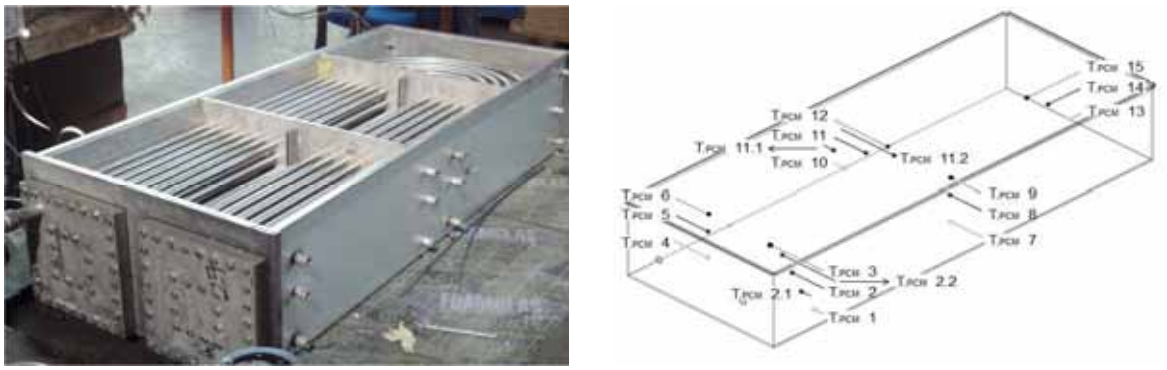

Fig. 6. Storage system. Left, shell-and-tubes concept; right, temperature sensors located inside the tank

5.1 Methodology

The experimentation carried out at the pilot plant is focused on a charging process at constant HTF temperature and flow rate. However, a complete cycle consisting of charging and discharging is done in order to study the behaviour of the material under the solidification process.

Before starting the charging process a warming period was performed in order to heat the HTF and PCM up to the set-point temperatures. Once the both the HTF and PCM inside the tank reached the desired initial temperatures, the charging process started until the desired final temperatures. The characteristics of the experimentation are shown in table 5.

Tab. 5: Characteristics of the experimentation carried out

Parameter	Units	Charging	Discharging
HTF flow rate	[kg/h]	1500	1500
	[L/h]	1650	1650
HTF inlet temperature	[ºC]	120	80
PCM initial temperature	[ºC]	80	120
PCM final temperature	[ºC]	120	80

5.2 Results and discussion

Figure 7 shows the temperature profile of the material located at the area where are placed the two most representative temperature sensors of the system during two processes of charging and one of discharging for a flow rate of 1650 L/h (See Figure 6) within a temperature range of 50-120 ºC.

The first charging process took place during the first hour of experimentation within a temperature range of 50-80 ºC. Only sensible heat storage is observed and the behaviour of both temperature profiles is the expected, reaching first the set-point temperature the material located close to the HTF inlet ($T_{PCM.2}$).

The second charging process took place for 3.2 h within a temperature range of 80-120 ºC and both sensible and latent heat storage are observed. It can also be seen to see that during this charging process the material located near the tank inlet reached the desired temperature faster than the rest of the material. Hence, it also finished before the melting process (99-110 ºC), being the average time to carry out this process of about 20-25 minutes.

Finally, during the discharging process, a very interesting phenomenon can be observed: the subcooling effect at pilot plant scale is clearly reduced if compared to the results obtained at laboratory scale

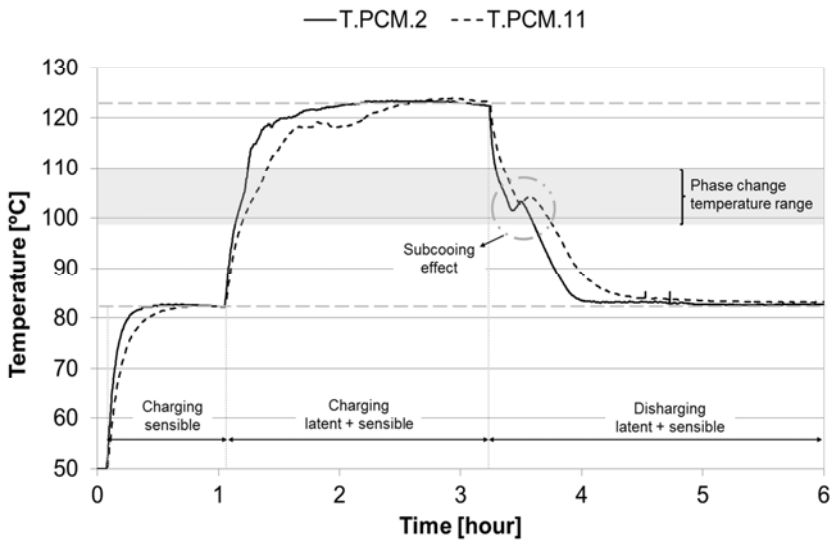

Fig. 7: PCM temperature profile with a flow rate of 1650 L/h for a temperature range of 50-120 ºC

Figure 8 shows the power given by the HTF to the system calculated according to eq. (1). The behaviour of the power given by the HTF is the expected, being higher at the beginning and decreasing along the time due to the variation in the HTF temperature gradient. As it can be seen, during the first hour it can be supplied up to more than 4 kW. Moreover, oscillations along the experiment are mainly due to the actuation of electronic controllers in the electrical boiler.

$$P_{HTF} = \dot{m}_{HTF} \cdot Cp_{HTF} \cdot (\pm T_{HTF.in} \pm T_{HTF.out}) \quad \text{(eq. 1)}$$

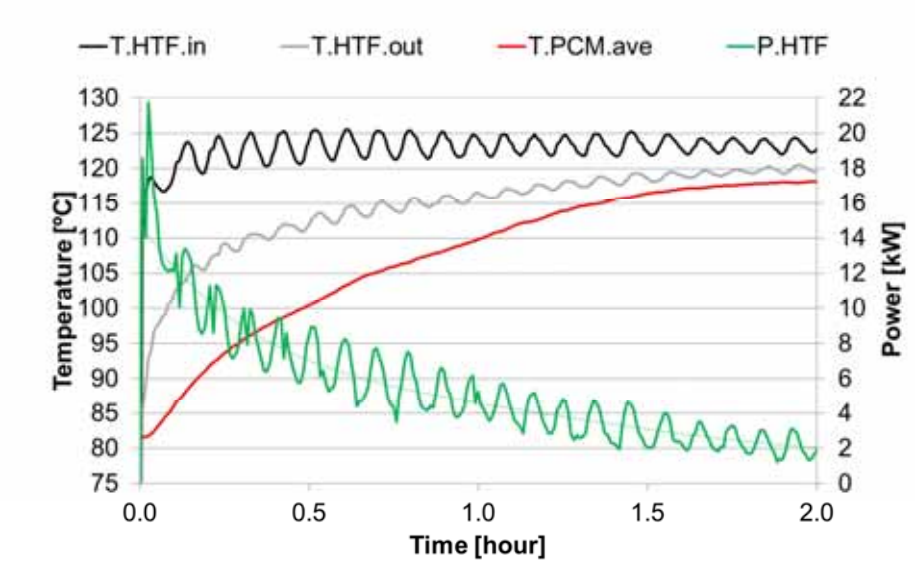

Fig. 8: HTF temperature profiles and power with a flow rate of 1650 L/h for a temperature range of 80-120 ºC

The energy balance equation that describes the processes performed in the present study can be written as eq. (2) shows:

$$\Delta E_{HTF} = \Delta E_{PCM} + \Delta E_{tank} + \Delta E_{insulation} + \Delta E_{loss} \quad \text{(eq. 2)}$$

where ΔE_{HTF} is the energy released by the HTF, ΔE_{PCM} is the energy stored by the TES storage material, ΔE_{tank} is the energy accumulated by the metallic parts of the tank, $\Delta E_{insulation}$ is the energy accumulated by the insulation and ΔE_{loss} is the energy lost from the tank to the environment.

Figure 9 shows the energy balance for the charging process. Notice that the energy released by the HTF at the end of the process (11.1 kWh) is higher than the stored by the PCM (9.9 kWh) with an efficiency of 89.2 % (eq. 3). Hence, the energy accumulated by the stainless steel of the tank (E_{tank}), accumulated by the insulation and the energy lost to the surroundings only represents 1.2 kWh.

$$\varepsilon_{char} = \frac{\Delta E_{PCM}}{\Delta E_{HTF}} \quad \text{(eq. 3)}$$

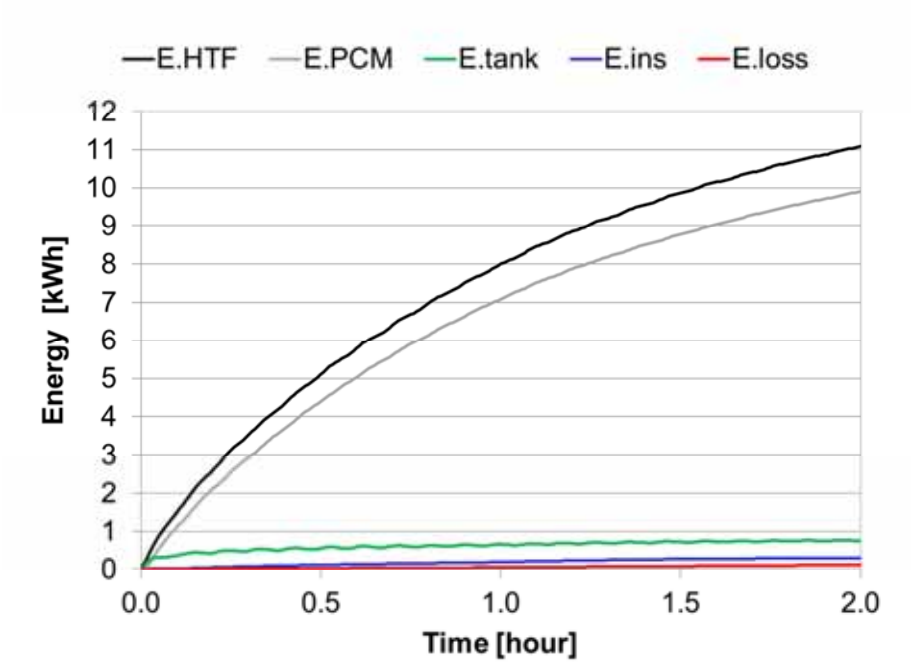

Fig. 9: Energy balance with a flow rate of 1650 L/h for a temperature range of 80-120 ºC

6 Conclusions

Bischofite is a by-product from the non-metallic industry composed mainly by $MgCl_2 \cdot 6H_2O$ in approximately 95%. The main advantage of the use of bischofite instead of $MgCl_2 \cdot 6H_2O$ is the price, which is significantly lower, and the availability.

Bischofite is first characterized at laboratory scale. Impurities of bischofite have been identified as potassium carnalite, lithium sulphate monohydrate, and ionic salts like NaCl and KCl. Viscosity and density was also determined for bischofite and $MgCl_2 \cdot 6H_2O$. Both materials show similar thermo-physical properties, the temperature and the heat of fusion is 100 °C and 115 kJ/kg for bischofite, and 114.5 °C and 135 kJ/kg for $MgCl_2 \cdot 6H_2O$. At pilot plant scale (≈ 250 kg), bischofite is charged from 80 to 120 ºC in a shell-and-tube heat exchanger. During the first hour of charging, the configuration used in the present study can supply up to more than 4 kW with a peak at the beginning of the experimentation of about 22 kW. For a total amount of 204 kg of bischofite and 2 hours of process, the energy released by the HTF is 11.1 kWh and the energy stored by the PCM 9.9 kWh, with an efficiency of 89.2 %. Notice that subcooling behaviour appearing in laboratory scale (37 ºC for bischofite and 29 ºC for $MgCl_2 \cdot 6H_2O$) disappears completely at pilot plant scale.

Moreover, this PCM candidate is also compared with other materials with similar melting temperature (± 20 ºC) regarding the cost and the energy density and a list of possible applications on IWH recovery is presented.

6. Acknowledgements

The authors want to thank Joan Tarragona Roig from the University of Lleida for his help during the experimental analysis in the pilot plant testing facility.
The work was partially funded by the Spanish government (project ENE2011-22722), by FONDECYT (grant N° 1120422), by CONICYT/FONDAP N°15110019 SERC-Chile, and the Education Ministry of Chile Grant PMI ANT 1201. The work leading to this invention has received funding from the European

Union's Seventh Framework Programme (FP7/2007-2013) under grant agreement n° PIRSES-GA-2013-610692 (INNOSTORAGE). The authors would also like to thank the Catalan Government for the quality accreditation given to their research group GREA (2014 SGR 123) and the collaboration of the company SALMAG. Laia Miró would like to thank the Spanish Government for her research fellowship (BES-2012-051861). Andrea Gutierrez would like to acknowledge to the Education Ministry of Chile her doctorate scholarship ANT 1106.

7. References

Brueckner, S., Liu, S., Miró, L., Radspieler, M., Cabeza, L.F., Laevemann E.,2014. Industrial waste heat recovery technologies: an economic analysis of heat transformation technologies. Submitted to Appl Energ.

Cabeza L.F., A. Castell, C. Barreneche, A. de Gracia, A.I. Fernández., 2011. Materials used as PCM in thermal energy storage in buildings: A review. Renew Sust Energ Rev.

Gil, A., Oró, E., Castell, A., Cabeza, L.F., 2013. Experimental analysis of the effectiveness of a high temperature thermal storage tank for solar cooling application. Appl Therm Eng.

International Energy Agency, 2014. Technology Roadmap: Energy storage.

Kenisarin M., Mahkamov K., 2007. Solar energy storage using phase change materials. Renew Sust Energ Rev.

Miró, L., Navarro, M.E., Suresh, P., Gil, A., Fernández, A.I., Cabeza, L.F., 2014. Experimental characterization of a solid industrial by-product as material for high temperature sensible thermal energy storage (TES). Appl Energ.

Sharma, A., Sharma S.D., Buddhi D., 2002. Accelerated thermal cycle test of acetamide, stearic acid and paraffin wax for solar thermal latent heat storage applications. Energ. Convers. Manage.

Stevens K., 2013. Integrated energy storage system for optimal energy production A case study on Johannes CHP biofuel plant. University of Gävle.

Ushak, S., Gutierrez, A., Galleguillos, H., Fernandez, A.G., Cabeza L.F., Grágeda, M., 2014. Thermophysical characterization of a by-product from the non-metallic industry as inorganic PCM. Submitted to Sol Energ Mat Sol C.